Stochastic method for calculating the ground-state one-body density matrix of trapped Bose particles in one dimension

Omri Buchman and Roi Baer*

Fritz Haber Center for Molecular Dynamics, Institute of Chemistry, The Hebrew University of Jerusalem, Jerusalem 91904, Israel

(Received 11 May 2017; published 20 September 2017)

The one-body density matrix (OBDM) is a fundamental contraction of the Bose-Einstein condensate wave function, encapsulating its one-body properties. It serves as a major analysis tool with which the condensed component of the density can be identified. Despite its cardinal importance, calculating the ground-state OBDM of trapped interacting bosons is a challenge and to date OBDM calculations have been published only for homogeneous systems or for trapped weakly interacting bosons. In this paper we discuss an approach for computing the OBDM based on a double-walker diffusion Monte Carlo random walk coupled with a stochastic permanent calculation. We here describe the method and study some of its statistical convergence and properties applying it to some model systems.

DOI: 10.1103/PhysRevA.96.033626

I. INTRODUCTION

Despite its importance for determining the structure and properties of boson systems, calculation of the ground-state one-body density matrix (OBDM) proves to be a daunting task. Most effort has gone to homogeneous systems where the OBDM has a simpler structure because its eigenfunctions, the plane waves compatible with the system size, are known in advance from symmetry [1–5]. However, for trapped systems, the OBDM is considerably more complicated and has been calculated exactly (near analytically) only for hard-core particles in harmonic traps [6,7] and numerically exactly only for weakly interacting systems [8]. Monte Carlo (PIMC) methods have been used for systems containing thousands of weakly interacting bosons trapped in a harmonic potential at finite temperatures [9], but PIMC calculations of the OBDM become exponentially more demanding as temperatures drop and interactions grow. Diffusion Monte Carlo, employing a variational Monte Carlo guiding function has also been used for studying systems of bosons in three dimensions at various densities from weak to intermediate strength [10,11]. However, the OBDM in these approaches is evaluated by an approximate expression, involving the variational and mixed estimators of the OBDM relying on the quality of the guiding function. This makes them inappropriate for strong interactions and additionally, they suffer from instabilities in the population control resulting from singularities in the local energy under the guiding function [12].

In this paper, we present a stochastic approach for the calculation of the ground-state OBDM for trapped strongly interacting bosons. Such computational methods are essential for analyzing systems of small to intermediate number of one-dimensional (1D) bosons in the strong interaction regime [13–17]. The formalism seems applicable to any number of dimensions but in this paper we describe and study the implementation to 1D bosons, which are challenging systems due to their strong correlation effects [18,19]. The method is based on a DMC random walk and employs a stochastic method for estimating the permanents required to calculate the OBDM . In Sec. II we describe the basic formalism, definitions, and techniques; in Sec. III we apply the method to systems of bosons trapped in a harmonic well where interaction strength is increased while keeping the trap potential fixed and then in double-well traps where interaction strength is increased while keeping the density of the system (nearly) fixed; summary and conclusions are given in Sec. IV.

II. METHOD

A. Basic notions

For D bosons of mass m_b in a trap potential $v(q)$ (q is the Cartesian position coordinate of a particle) interacting through a pairwise potential $u(q_{12})$, the Hamiltonian is written as a sum of kinetic and potential energies:

$$\hat{H} = \hat{T} + \hat{V}, \tag{1}$$

$$\hat{T} = -\frac{\hbar^2}{2m_b}\sum_{n=1}^{D}\nabla_n^2 \tag{2}$$

$$\hat{V} = \sum_{n=1}^{D} v(q_n) + \sum_{m<n}^{D} u(|q_n - q_m|), \tag{3}$$

where $\hat{V}$ is a sum of one-body and two-body interactions. Although the formalism we develop is not limited to any specific form of the trap potential or two-body interactions, we will use, for demonstration purposes, the following even-symmetric trap, which combines a harmonic well with a Gaussian-shaped barrier in its center:

$$v(q) = \frac{1}{2}m_b\omega^2 q^2 + V_b e^{-\frac{q^2}{2\sigma_b^2}}. \tag{4}$$

Here ω, V_b, and σ_b are, respectively, the harmonic frequency, barrier height, and barrier width. The interaction we consider is a pairwise Gaussian repulsion of the form,

$$u(q_{12}) = \frac{c}{\sqrt{2\pi}\sigma_r} e^{-\frac{q_{12}^2}{2\sigma_r^2}}, \tag{5}$$

*roi.baer@huji.ac.il

where c is the repulsion strength and σ_r the interaction range. When addressing the purely harmonic trap ($V_b = 0$) we will use two pure quantities for characterizing the trap:

$$\alpha_0 = \frac{c}{E_0 l}, \tag{6}$$

$$\alpha_1 = \frac{\sigma_r}{l}, \tag{7}$$

where $E_0 = \hbar\omega$ and $l = \sqrt{\frac{\hbar}{m_b\omega}}$ are the energy and length scales of the single particle noninteracting harmonic ground state. Another nondimensional parameter comes from the theory of nontrapped 1D gases interacting via a δ-function potential ($\sigma_r \to 0$), involving the 1D scattering length $2\hbar^2/m_b c$ (see for example Ref. [20]):

$$\alpha_2 = \frac{\hbar^2}{m_b c l}. \tag{8}$$

Small values of α_2 mean that scattering events occur on a length scale smaller than the width of the trap. In the examples we give below almost all cases are within this regime.

The ground-state one-body density matrix (OBDM) for D bosons is defined up to a constant factor as an expectation value of a nonlocal operator:

$$\Gamma_1(q,\tilde{q}) \propto \int d\boldsymbol{x} d\tilde{\boldsymbol{x}} \Psi(\boldsymbol{x})\Psi(\tilde{\boldsymbol{x}}) \times \delta(x_1 - q)\delta(\tilde{x}_1 - \tilde{q}) \prod_{j=2}^{D} \delta(x_j - \tilde{x}_j), \tag{9}$$

where $\Psi(\boldsymbol{x}) \equiv \Psi(x_1, \ldots, x_D)$ is the ground state, symmetric to particle exchange and normalization $\int \Gamma_1(q,q)dq = D$ can be imposed *a posteriori*. Singling out particle 1 in this definition is arbitrary as all particles are identical. In fact, we can take advantage of the wave function exchange symmetry and write the OBDM in an equivalent but explicitly fully symmetric way:

$$\Gamma_1(q,\tilde{q}) \propto \int d\boldsymbol{x} d\tilde{\boldsymbol{x}} \Psi(\boldsymbol{x})\Psi(\tilde{\boldsymbol{x}}) \times \sum_j w(\boldsymbol{y}(\boldsymbol{x}|j), \boldsymbol{y}(\tilde{\boldsymbol{x}}|j))\delta(x_j - q)\delta(\tilde{x}_j - \tilde{q}), \tag{10}$$

where $\boldsymbol{y}(\boldsymbol{x}|j) \equiv (y_1, \ldots, y_{D-1}) = (\ldots, x_{j-1}, x_{j+1}, \ldots)$ is the vector of $D-1$ coordinates obtained from the vector $\boldsymbol{x}$ by removing the jth coordinate. The weight $w(\boldsymbol{y}, \tilde{\boldsymbol{y}})$ of each double configuration $\boldsymbol{y}$, $\tilde{\boldsymbol{y}}$ is the number of permutations P of the $\tilde{y}$ coordinates having the property that simultaneously for all k, the position $\tilde{y}_{P_k}$ is located in an infinitesimal volume element surrounding the position of y_k. Mathematically this is expressed as the following sum of products of δ functions: $w(\boldsymbol{y}, \tilde{\boldsymbol{y}}) \equiv \sum_P \prod_k \delta(y_k - \tilde{y}_{P_k})$.

For a numerical implementations, we coarse-grain the δ functions. First, we introduce a q-axis grid containing $2N_G$ bins, each of width h, centered on the grid points $y_g = gh$, where $g = -N_G, -N_G, +1, \ldots, N_G - 1, N_G$ is an integer. The coarse-grained OBDM is then a histogram on a $2N_G \times 2N_G$ lattice derived from the exact OBDM as an integral over the bins:

$$\Gamma_1^{g\tilde{g}} \equiv h^{-2} \iint \Gamma_1(q,\tilde{q})\theta_h(q - y_g)\theta_h(\tilde{q} - y_{\tilde{g}})dqd\tilde{q}, \tag{11}$$

where $\theta_h(\xi)$ equals 1 if $\xi \in [-\frac{h}{2}, \frac{h}{2}]$ and zero otherwise.

Next we introduce the DMC random walk as a means for calculating the coarse-grained OBDM. Regular DMC produces a trajectory of length N_T time steps made by M walkers, giving $M \times N_T$ D-dimensional vectors $\boldsymbol{x}$ distributed as the ground-state wave function $\Psi(\boldsymbol{x})$. However, this is not what we need for the OBDM of Eq. (10), where the integral is over $\Psi(\boldsymbol{x})\Psi(\tilde{\boldsymbol{x}})$. Hence we apply the standard DMC procedure not on a single but on a double-walker system corresponding to $2 \times D$ particles under the Hamiltonian $\hat{H} = \hat{H}(\boldsymbol{x}) + \hat{H}(\tilde{\boldsymbol{x}})$, producing a random walk trajectory of $M \times N_T$ $2D$-dimensional vectors $(\boldsymbol{x}, \tilde{\boldsymbol{x}})$ distributed as the product of ground-state wave functions $\Psi(\boldsymbol{x})\Psi(\tilde{\boldsymbol{x}})$. The coarse-grained OBDM histogram then becomes equal (up to normalization) to the following average along such a trajectory:

$$\Gamma_1^{g\tilde{g}} \propto \left\langle \sum_j w_h(\boldsymbol{y}(\boldsymbol{x}|j), \boldsymbol{y}(\tilde{\boldsymbol{x}}|j))\theta_h(x_j - y_g)\theta_h(\tilde{x}_j - y_{\tilde{g}}) \right\rangle_{M \times N_T}, \tag{12}$$

where

$$w_h(\boldsymbol{y}, \tilde{\boldsymbol{y}}) = \sum_P \prod_k \theta_h(y_k - \tilde{y}_{P_k}) \tag{13}$$

are the coarse-grained weights. The sum over the permutations is not required when the random walk continues indefinitely, producing exhaustive sampling [we can take $w_h(\boldsymbol{y}, \tilde{\boldsymbol{y}}) = 1$]. However, sampling is evidently finite, and not taking the permutations will result in extremely poor statistics because of the small probability to find y_k and $\tilde{y}_k$ in the same bin simultaneously for all $k = 1, \ldots, D$. The sum of products over permutations appearing in Eq. (13) is the formal definition of a permanent of the $(D-1) \times (D-1)$ matrix describing the adjacency of particles in the two components of the double walker:

$$\Theta_{kj} = \theta_h(y_k - \tilde{y}_j). \tag{14}$$

Note that the expression of the permanent in Eq. (13) is almost identical to that of the determinant except that in the latter all odd permutations P are multiplied by -1. Despite this similarity, the numerical work needed to evaluate the permanent is vastly larger than for the determinant: the former involves exponential complexity, $O(2^D D)$ [21], while the latter is polynomial, $O(D^3)$. For this reason, we use a stochastic method [22] for evaluating the permanent in polynomial time, as discussed in the following algorithm.

B. Algorithm for calculating the one-body density matrix

The M DMC double walkers $(\boldsymbol{x}_m, \tilde{\boldsymbol{x}}_m)$ $(m = 1, \ldots, M)$ are subject to the standard DMC diffusion and birth and/or death processes in a series of N_T time steps, each of duration Δt, depending on the Hamiltonian $\hat{H}(\boldsymbol{x}) + \hat{H}(\tilde{\boldsymbol{x}})$ as follows.

(1) Diffusive step: the position of each walker is changed by $(\Delta\boldsymbol{x}_m, \Delta\tilde{\boldsymbol{x}}_m)$, a vector of random numbers, each sampled

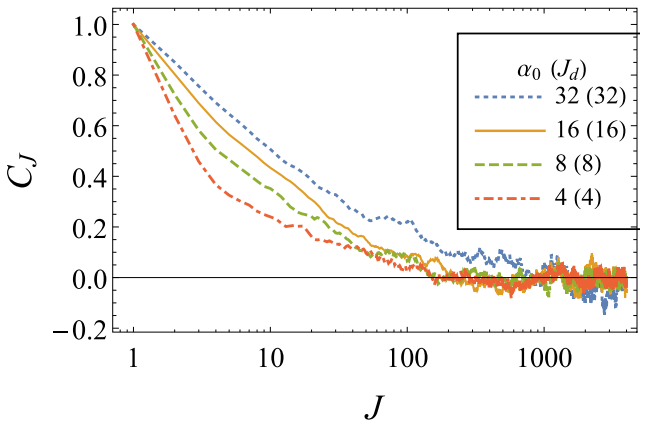

FIG. 1. The autocorrelation function $C_J = \sum_m (E_{J+m} - \bar{E})(E_m - \bar{E})/\sum_m (E_m - \bar{E})^2$, where E_m is the DMC reference energy at time step m and $\bar{E}$ is its mean, for $D = 16$ bosons in a harmonic oscillator trap for several values of α_0 (and $\alpha_1 = 0.1$). The decay constant J_d (defined by $C_{J_d} = e^{-1} \approx 0.37$) is indicated in parentheses. Interestingly, in each case the value of J_d is approximately equal to α_0.

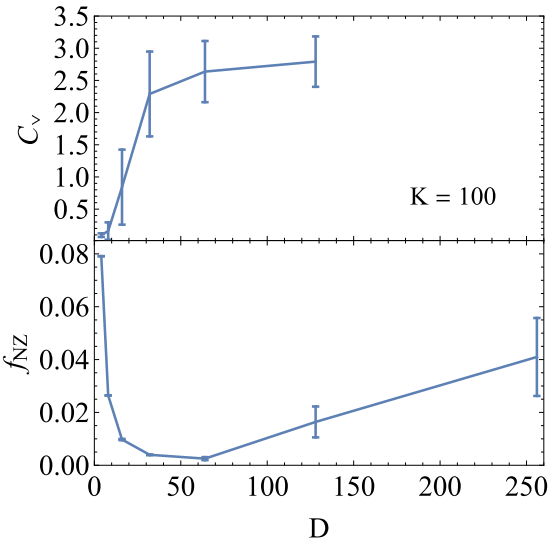

FIG. 2. The application of the stochastic permanent evaluation described in step 4b of the algorithm in Sec. II B to adjacency matrices Θ_{ij} [Eq. (14)] appearing in DMC trajectories corresponding to D interacting bosons inside a Harmonic well [$\alpha_0 = 4, \alpha_1 = 0.1$ in Eqs. (6)–(7)]. Top: The coefficient of deviation C_v (relative standard deviation) for the stochastic permanent evaluation as a function of D. For each adjacency matrix Θ, the permanent is reevaluated stochastically ten times (every time using $K = 100$ sets of random integers) and $C_v(\Theta)$ is calculated as the ratio of the standard deviation to the average. The results shown in the figure are averages $\langle C_v(\Theta)\rangle$ over 10000 instances of Θ matrices, which arise during the DMC random walk. Bottom: The frequency of nonzero permanents as a function of D.

from the normal distribution with mean $\mu = 0$ and variance $\sigma^2 = \frac{\hbar\Delta t}{m_b}$.

(2) Reproduction/annihilation: For each walker at time t, $(\boldsymbol{x}_m, \tilde{\boldsymbol{x}}_m)$, an integer $n = INT[e^{(E(t)-[V(\boldsymbol{x}_m)+V(\tilde{\boldsymbol{x}}_m)])\Delta t/\hbar + M - M_0} + r]$ is computed (where M_0 is a preset target number of walkers), $0 \leqslant r < 1$ is a random fraction and $E(t) = \frac{1}{M}\sum_{k=1}^{M}[V(\boldsymbol{x}_k) + V(\tilde{\boldsymbol{x}}_k)]$ is the average potential energy over all walkers at time step $t = 1, \ldots, N_T$. Then:

(a) if $n > 0$ n clones of the walker are generated and M is increased by n

(b) if $n = 0$ the walker is eliminated and M is decreased by 1.

(3) Evaluating the energy: In the appropriate limit ($M \to \infty$, $\Delta t \to 0$, and $N_T \to \infty$) the expected time-step average of $E(t)$ is an unbiased estimate of the ground-state energy of the double system:

$$2E_{GS} = \left\langle \frac{1}{N_T}\sum_{n=1}^{N_T} E(n\Delta t) \right\rangle, \tag{15}$$

and the $M \times N_T$ walker positions $(\boldsymbol{x}, \tilde{\boldsymbol{x}})$ are distributed as $\Psi(\boldsymbol{x})\Psi(\tilde{\boldsymbol{x}})$. The numerical procedure uses a finite number M of walkers, a finite time step Δt, and a finite number of sampling times N_T, leading estimates of E_{GS} having random fluctuations $\Sigma_{(M,N_T)} \propto \frac{1}{\sqrt{N_T M}}$ as well as a small bias due to the finite time step Δt.

(4) Estimating the OBDM: Every N_C time steps the DMC double walkers are used update the OBDM histogram according to Eq. (12). N_C is taken much larger than the correlation decay lengths J_d of the walk (see Fig. 1). In Eq. (12), the bosonic weight $w_h(\boldsymbol{y}, \tilde{\boldsymbol{y}})$ is equal to the permanent of the $(D-1)\times(D-1)$ adjacency matrix Θ_{ij} of Eq. (14), which is evaluated following these steps:

(a) Preliminary screening: we compute the column sums $c_j = \sum_{i=1}^{D}\Theta_{ij}$ and the row sums $r_i = \sum_{j=1}^{D}\Theta_{ij}$ of the adjacency matrix and if one of these is zero the permanent is immediately set to zero without further computation. The numerical effort in this screening process scales at most as $O(D^2)$ and is effective since typically only a small fraction of the permanents are nonzero (see bottom panel of Fig. 2).

(b) For the adjacency matrices passing step 4a, the permanent is estimated as the average $\langle|\det\Phi|^2\rangle$ where Φ is the matrix obtained from Θ by multiplying each of its elements by ± 1 at random. Mathematically, $\Phi_{ij} = (-)^{n_{ij}}\Theta_{ij}$ where n_{ij} are random independent integers [22]. The average $\langle|\det\Phi|^2\rangle$ is estimated using K samples of the integers n_{ij}, where K is on the order of a few hundreds. The relative standard deviation C_v occurring in this stochastic permanent evaluation for a typical DMC trajectory is shown in the top panel of Fig. 2 for $K = 100$. C_v grows roughly in proportion to D, for large D's.

(c) Normalize ($\Gamma_1^{g\tilde{g}} \leftarrow \Gamma_1^{g\tilde{g}} \times \frac{D}{tr\Gamma_1 h^2}$) and symmetrize [$\Gamma_1^{g\tilde{g}} \leftarrow (\Gamma_1^{g\tilde{g}} + \Gamma_1^{\tilde{g}g})/2$] the completed OBDM histogram of Eq. (12).

We found the statistical error Σ_{RDM} of any OBDM property we looked at (eigenvalues, for example) is proportional to $\frac{1}{\sqrt{N_T M K}}$ where N_T is the number of time steps, M the number of walkers and K the number of determinants used in the permanent evaluation. From this, we conclude that the bias, if it exists, is small and the error is dominated by statistical fluctuations.

The algorithm quickly identifies most of the zero permanents, however, it is clear that for the sampling to be efficient

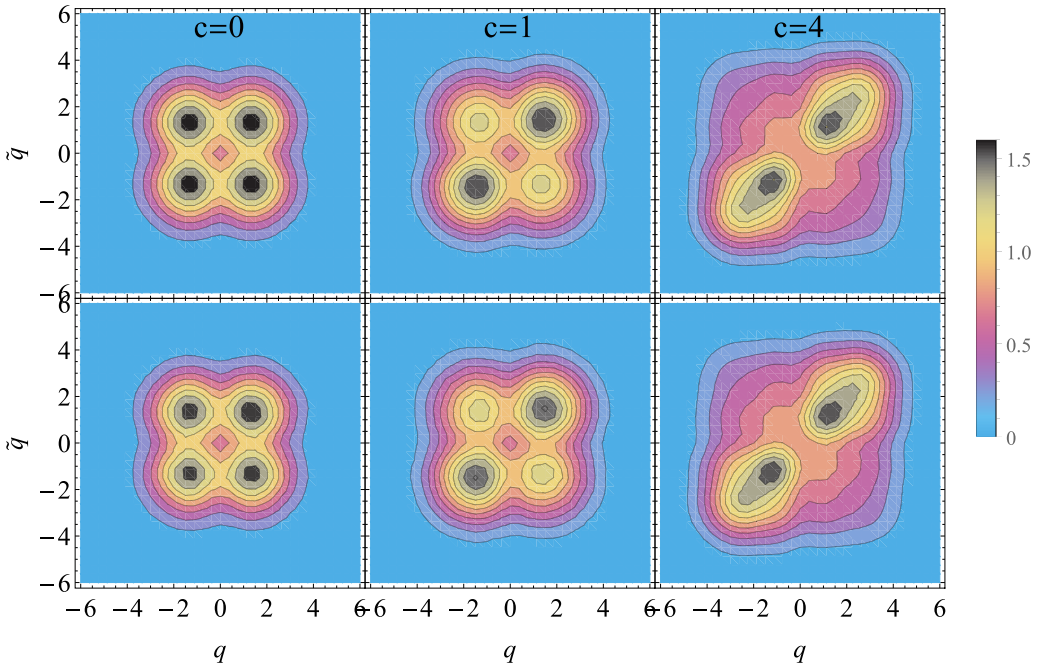

FIG. 3. The deterministic (top) and DMC (bottom) OBDM $\Gamma_1(q,\tilde{q})$ for of $D = 4$ unit-mass particles trapped in the potential well $v(x)$ of Eq. (4) and interacting via the potential $u(x_{12})$ of Eq. (5). The parameters are $k_H = 0.25$, $V_b = 1.5$, $\sigma_b = 0.5$, and $\sigma_r = 0.5$ and the values of c are indicated in the figure for each column. A bin size of $h = 0.375$ atomic units was used for sampling. The DMC calculation used a total of $M = 48000$ walkers (128 000 for $c = 4$), $N_T = 4000$ time steps (20000 for $c = 4$), and $\Delta t = 0.01$ time units (0.005 for $c = 4$).

we cannot afford a situation where the permanents are rarely different than zero. Hence, the bin size h should not be too small, and a general rule of the thumb would be to take h to be of the order of n^{-1} (or a small fraction thereof) where n is the average density. The efficacy of the permanent method is seen in that the fraction of nonzero permanents grows with increasing number of particles for a Harmonic traps (see bottom panel of Fig. 2). This finding has support of theoretical investigations [23]. Thus, the sampling efficiency is not expected to decrease and perhaps even increases as the number of particles grows.

C. Statistics and validation

In Fig. 3 we show contour plots of a grid-based deterministic and the DMC-based stochastic OBDM estimates of $\Gamma_1(q,\tilde{q})$ for several systems of $D = 4$ particles interacting with increasing repulsion strengths. In each case the DMC-based and grid-based OBDMs are indeed nearly identical in appearance, due to extensive sampling, validating, in principle, our method.

To show the effect of the stochastic permanent evaluation, we study the three highest-lying OBDM eigenvalues for a set of 16 bosons in a Harmonic trap, as shown in Table I. The averages and fluctuations using DMC with deterministic permanent evaluation and DMC with stochastic permanent evaluation for $K = 200$ and 400 stochastic determinants are shown. The expectation values are close and the standard deviations with $K = 400$ are close to the deterministic fluctuations.

III. APPLICATIONS

In this section we apply the algorithm for two types of trapped boson systems in order to demonstrate the performance and the kind of results that can be obtained. We compare the calculated densities to that of the Thomas-Fermi (TF) approximation [24,25], given as the positive part of the shifted and negatively scaled potential well:

$$n_{TF}(q) = \mathcal{P}\frac{\mu - v(q)}{c}. \tag{16}$$

where P symbol means only positive values are nonzero. Here, the TF chemical potential μ is determined by the density normalization condition $\int n_{TF}(q)dq = D$.

A. Constant harmonic-well trap

In Fig. 4 we study 16 trapped bosons in a harmonic well as a function of α_0, taking the values 4, 8, 16, 32 with $\alpha_1 = 0.1$ and

TABLE I. The expected value and standard deviation of the three largest OBDM eigenvalues for a system of 16 bosons in a Harmonic trap, calculated using DMC comparing the deterministic ($K = 0$) and stochastic ($K = 200, 400$) evaluations of permanents. The parameter K is the number of stochastic determinant calculations used for each permanent evaluation. The potential parameters [see Eqs. (6)–(7)] are $\alpha_0 = 4$, $\alpha_1 = 0.1$. The DMC calculation used $M = 64000$ walkers and $N_T = 8000$ time steps with $\Delta t = 0.005\omega^{-1}$ and the OBDM bin size was $h = 0.625$.

	0		200		400	
K	$E(f)$	$\sigma(f)$	$E(f)$	$\sigma(f)$	$E(f)$	$\sigma(f)$
f_1	0.806	0.01	0.808	0.014	0.805	0.008
f_2	0.085	0.006	0.086	0.009	0.085	0.007
f_3	0.047	0.006	0.043	0.003	0.047	0.006

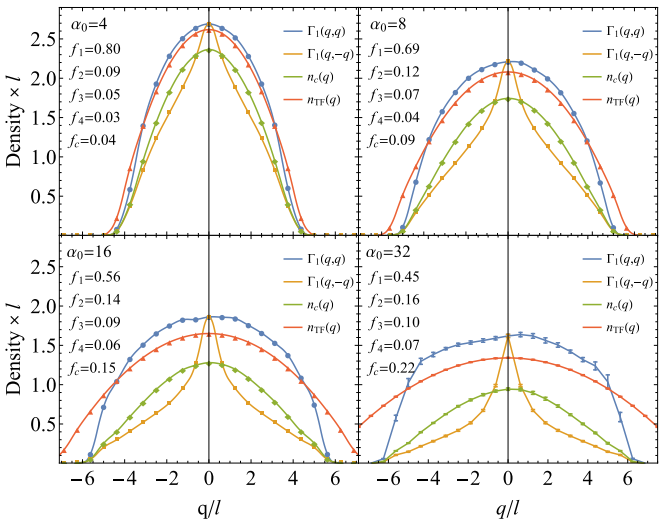

FIG. 4. The OBDM diagonal, antidiagonal, condensate $[n_C(q)]$, and Thomas-Fermi $[n_{TF}(q)]$ densities for $D = 16$ particles in a Harmonic well interacting via the potential of Eq. (5). The interaction range parameter is $\alpha_1 = 0.1$ while the interaction strength parameter α_0 is indicated in the panels. The OBDM eigenvalues (divided by D) are the eigenstate fractions f_n indicated in each panel with f_1 and f_2 having relative errors of 10% and f_3 and f_4 of 20% (largely independent of α_0). For $\alpha_0 < 32$ the statistical error bars are not larger than the marker symbols. For $\alpha_0 = 32$ the statistical error bars are shown explicitly for the diagonal, antidiagonal and condensate densities. The OBDM bin size was $h = 0.625$.

$V_b = 0$ (corresponding DMC run parameters given in Table II). We choose the regime of small α_1 so the interaction is close to contact. A useful way to think of this series of systems is to imagine that the repulsion strength c increases (in proportion to α_0) while the harmonic trap stays put.

It is seen that as the repulsion (α_0) grows, the density diminishes and broadens. This happens because at short inter particle distances the repulsion force is stronger than the harmonic force and thus, as repulsion grows the particles can stretch the harmonic spring and spread out.

For $\alpha_0 = 4$ and 8 the density $\Gamma_1(q,q)$ in Fig. 4 is similar in shape to the TF density $n_{TF}(q)$ [Eq. (16)]. The TF approximation is expected to apply for large numbers of particles [18], and weak interactions $\alpha_0 \ll 1$, and is seen here to work surprisingly well beyond this limit. As α_0 increases further, the system gradually assumes a more Fermionic structure, which includes a flattening of the density profile. However, the TF density retains the parabolic shape and therefore is not any more a reasonable approximation to the density.

As for the condensate density $n_c(q)$. For the lowest value $\alpha_0 = 4$, it is very similar in shape to the total density, just scaled by a factor $f_1 \approx 0.8$ where f_1 is the condensate fraction. As α_0 increases the condensate is gradually destroyed. This is evidenced by the steady decrease of the condensate fraction f_1 and then by the antidiagonal density $\Gamma_1(q,-q)$, progressively developing a concave shorter-ranged character while deviating in shape from the total density $\Gamma_1(q,q)$ (see Appendix for discussion). Finally as interactions grow, the shape of the condensate density $n_c(q)$, retaining its flexible smoothness, increasingly deviates from that of the total density, which displays increasing rigidity due to fermionization.

Figure 4 also displays the statistical error bars for the $\alpha_0 = 32$ system. It is seen that the total density is considerably more sensitive to the QMC statistical fluctuations than the condensate density (and the antidiagonal density). This is reminiscent of the two-fluid model of superfluid He-II [26] according to which the condensate has vanishing viscosity and therefore is immune to fluctuations quite distinct from the behavior of the normal fluid.[1]

TABLE II. The parameters for the DMC runs used to produce the results shown in Fig. 4. The wall time in hours and the number of core-i7 CPU's used (each CPU running eight threads).

	α_0			
DMC run data	4	8	16	32
M ($\times 10^3$)	96	96	480	640
N_T ($\times 10^3$)	900	900	900	6000
N_J	250	250	500	500
K	100	100	100	100
$\omega\Delta t$ ($\times 10^{-3}$)	5	2.5	2.5	2.5
Wall time hrs × CPU	11 × 3	10 × 3	33 × 6	192 × 8

B. Constant density in double-well trap

The generality of the DMC-based OBDM calculation allows us to study systems beyond the uniform gas and the harmonic trap approximations. One interesting case, is the partially fragmented trapped gas, which is formed in a double-well potential. When the barrier is extremely wide and tall, the system fragments into two condensates [27,28] with OBDM exhibiting two large and equal eigenvalues. However, if the barrier is only partially separating the condensate the nature of the system is mixed and difficult to describe without detailed calculation.

Here we examined the behavior of the bosons when trapped in a double well as the repulsion strength is increased. If we keep the trap potential unchanged while increasing steadily the repulsion constant c, the boson cloud will expand and deplete in density, its potential energy will grow, until the effect of the double-well potential barrier will be but a small perturbation. In order to prevent this, we examine in Fig. 5 systems of increasing repulsion constant c while at the same time changing the trap [spring constant k_H and barrier height V_b in Eq. (4)] so that the boson density remains unchanged. This is a different limit than that studied in the previous section, where we kept the trap constant as we increased c and the density decreased. This limit is relevant to the density functional theory of Bose gases where it can be combined with the adiabatic connection theorem to calculate the exchange-correlation energy [29,30].

We found that with constant $\sigma_r = 0.1$ and $\sigma_b = 0.5$, the TF density is unchanged if we preserve the ratios V_b/c and k_H/c (we took these equal to 3 and 2.86, respectively). The OBDM properties of four such systems with $c = 2$, 4, 8, and

[1]The viscosity of a fluid is related to momentum fluctuations by the Green-Kubo formula.

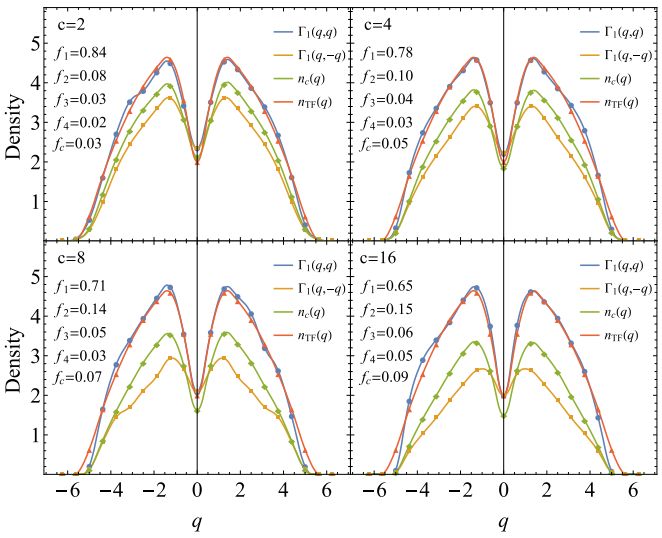

FIG. 5. The OBDM diagonal, antidiagonal, condensate $[n_C(q)]$, and Thomas-Fermi $[n_{TF}(q)]$ densities for $D = 32$ particles with the value of c indicated in the panels and $\sigma_r = 0.1$, $\sigma_b = 0.5$. The other two potential parameters are taken as $k_H = 2.86c$ and and $V_b = 3c$. This forces the TF density to be identical in all four systems. The OBDM eigenstate fractions $f_n, n = 1, \ldots, 4$ as well as $f_c = \sum_{n>4} f_n$, are indicated in each panel; f_1 and f_2 have relative errors of 10% and f_3 and f_4 of 20% (largely independent of c). The DMC parameters are given in Table III. The bin size was $h = 0.625$ (all quantities are unit less).

16 are shown in (5), (corresponding DMC run parameters given in Table III). Since the density is kept constant the main response is expressed as off diagonal changes in the OBDM as c grows. What we see is that the antidiagonal $\Gamma_1(q,-q)$ gradually diminishes for intermediate values of q and deforms, smearing the double-hump feature. The condensate density, like the total density $\Gamma_1(q,q)$, seems to preserve its shape but reduces as contributions from other eigenfunctions of the OBDM grow. Indeed, the strengthening of c reduces the value of the condensate fraction, i.e., the largest OBDM eigenvalue fraction, from $f_1 = 0.84$ at $c = 2$ to $f_1 = 0.65$, while compensating by increasing the other eigenvalue fractions f_2, f_3, and f_4. Note that the growing value of the sum of higher-state population fractions $f_c = \sum_{k>4} f_k$, reaching 9% at $c = 16$. The second eigenvalue does not grow appreciably larger than the third or fourth eigenvalue fractions, showing that the condensate is not fragmented despite the visibly deep cut through the density at $x = 0$.

TABLE III. The parameters for the DMC runs ($D = 32$ bosons in a double well, keeping the density constant as the interaction constant c grows) used to produce the results shown in Fig. 5. The wall-time in hours and the number of core-i7 CPU's used (each CPU running 8 threads). The DMC correlation time for $c = 16$ was large and required large N_J to reduce fluctuations.

	c			
DMC run data	2	4	8	16
M ($\times 10^3$)	256	256	256	512
N_T ($\times 10^3$)	75	140	250	350
N_J	50	100	250	500
K	100	100	100	100
$N_{\text{det}} = MN_TK/N_J$ ($\times 10^{10}$)	3.8	3.6	2.6	3.6
$\omega\Delta t$ ($\times 10^{-3}$)	1.25	1.25	1.25	1.25
Wall time hrs × CPU	64 × 4	65 × 4	53 × 4	47 × 8

IV. SUMMARY AND DISCUSSION

In this paper we have developed a stochastic method for calculating the OBDM of trapped Bose particles in the ground state. The method is based on a unguided DMC process in which a double walker is used to estimate the OBDM $\Gamma_1^{q\tilde{q}}$ (where q designates bins on the position axis) as a permanent of the double-walker adjacency matrix. We have used the method to treat systems of up to 32 bosons with usefully converged statistics in harmonic and double-well traps. Based on the tests we ran, we estimate the complexity to scale as $D^6 = D^3 \times D^2 \times D$ where the first factor is due to the complexity of a determinant calculation, the second is our estimate of the increase in the number of determinant evaluations needed for each permanent calculation due to the linear increase of the relative statistical fluctuations C_v with D (top panel of Fig. 2) and the third is due to the fact that for each double walker we repeat the permanent evaluation D times. In a limited range of D, the efficiency of the sampling decreases with increasing D due to the decrease in the number of nonzero permanents (see the bottom panel of the figure). However, when D grows further this effect will diminish since the fraction of nonzero permanents actually grows with D. In calculating the OBDM of harmonically trapped particles with $\alpha_0 = 4$ and $\alpha_1 = 0.1$, the CPU time increased by a factor ~50 when going from $D = 16$ to $D = 32$ (keeping the same level of statistical fluctuations), which is consistent with this scaling. Note, however, that this estimated complexity is based on experience with the Harmonic-trapped Bosons and short interaction ranges. Its generality needs to be further investigated tested in different settings and applications.

It is tempting to compare the computational complexity of the present OBDM calculation method with that of other published methods. The most serious contender is the path integral ground-state method [2–4], which has been applied to calculation of the OBDM from the weakly to the strongly interacting regimes [5] However, although formulated in a general way, this approach been applied only for homogeneous systems where the OBDM is a function of the displacement $\Delta q = q - q'$ and thus greatly benefits from averaging over the coordinate q, an advantage that cannot be exploited in trapped (nonhomogeneous) systems.

We point out that while in this paper we focused on short-ranged repulsive 1D particles, there is no formal reason why the method will not be applicable for higher dimensions and other types of interactions. Indeed the possibility of these issues is left as future directions.

It is important to appreciate that the present stochastic OBDM calculation essentially involves a stochastic postprocessing step placed on top of a DMC random walk. As such, the same technique can perhaps be used in conjunction with other types of Monte Carlo methods or even with deterministic approaches that produce a wave function. This too is a possible direction for extending the method.

ACKNOWLEDGMENT

This work was funded by Israel Science Foundation under Grant No. 189/14.

APPENDIX: OBDM DIAGONAL AND ANTI-DIAGONAL FOR POTENTIALS WITH INVERSION SYMMETRY

The condensate is associated with the antidiagonal long range of the density matrix [31,32]. In finite systems it is more difficult to speak of long range yet the relation, e.g., ratio, of the antidiagonal and diagonal can be considered. We describe this approach here.

For the OBDM of the (non-negative) ground state, as considered here, the OBDM $\Gamma_1(q,\tilde{q})$ is also manifestly non-negative. Furthermore, if the trap potential is symmetric $v(q) = v(-q)$, the OBDM eigenstates $\psi_n(q)$ [$\Gamma_1(q,\tilde{q}) = \sum_n w_n \psi_n(q)\psi_n(\tilde{q})$ where $1 \geqslant w_n \geqslant 0$ are the OBDM eigenvalues] are either symmetric or antisymmetric to inversion. The diagonal and antidiagonal densities can thus be written as

$$\Gamma_1(q,q) = \sum_n w_n |\psi_n(q)|^2 \tag{A1}$$

$$\Gamma_1(q,-q) = \sum_{\psi\in\text{even}} w_n |\psi_n(q)|^2 - \sum_{\psi\in\text{odd}} w_n |\psi_n(q)|^2. \tag{A2}$$

Focusing on the sum and difference between the OBDM diagonal $\Gamma_1(q,q)$ and antidiagonal $\Gamma_1(q,-q)$, we define two non-negative even/odd (+/−) state densities

$$n_\pm(q) = \tfrac{1}{2}[\Gamma_1(q,q) \pm \Gamma_1(q,-q)], \tag{A3}$$

and the corresponding even/odd populations $D_\pm = \int n_\pm(q)dq$. Clearly, the sum $D_+ + D_- = \int \Gamma_1(q,q)dq$ is the total population D, while the difference,

$$D_+ + D_- = \int \Gamma_1(q,-q)dq \tag{A4}$$

is the integral of the antidiagonal (which is thus always positive). Since the densities $n_+(q)$ and $n_-(q)$ are positive, the OBDM diagonal is never smaller than its antidiagonal and so the ratio $1 \geqslant \Gamma_1(q,-q)/\Gamma_1(q,q)$ is well defined. The presence of a condensate can perhaps be associated with a bound of this ratio from below as q grows:

$$a < \Gamma_1(q,-q)/\Gamma_1(q,q). \tag{A5}$$

Equality of diagonal and antidiagonal happens when only even states are populated. One such case is for the noninteracting Bose gas in its ground state, where only the (even) ground state is populated, in this case $D = D_{\text{even}}$ and $D_{\text{odd}} = 0$. Once a noncondensate is formed (due to interactions or increase of temperature, for example) some of population is transferred into odd states and therefore $D_{\text{even}} - D_{\text{odd}}$ diminishes. From Eq. (A4) this latter effect causes the reduction of the OBDM antidiagonal integral $\int \Gamma_1(q,-q)dq$. All the while, the diagonal integral $\int \Gamma_1(q,q)dq$, remains equal to D. For this reason, a small antidiagonal population is indicative of a large noncondensate being formed.

[1] D. M. Ceperley, Rev. Mod. Phys. **67**, 279 (1995).
[2] A. Sarsa, K. Schmidt, and W. Magro, J. Chem. Phys. **113**, 1366 (2000).
[3] E. Vitali, M. Rossi, F. Tramonto, D. E. Galli, and L. Reatto, Phys. Rev. B **77**, 180505(R) (2008).
[4] M. Rossi, M. Nava, L. Reatto, and D. Galli, J. Chem. Phys. **131**, 154108 (2009).
[5] R. Rota, F. Tramonto, D. E. Galli, and S. Giorgini, Phys. Rev. B **88**, 214505 (2013).
[6] M. D. Girardeau, E. M. Wright, and J. M. Triscari, Phys. Rev. A **63**, 033601 (2001).
[7] T. Papenbrock, Phys. Rev. A **67**, 041601 (2003).
[8] K. Sakmann, A. I. Streltsov, O. E. Alon, and L. S. Cederbaum, Phys. Rev. A **78**, 023615 (2008).
[9] W. Krauth, Phys. Rev. Lett. **77**, 3695 (1996).
[10] J. L. DuBois and H. R. Glyde, Phys. Rev. A **68**, 033602 (2003).
[11] G. Astrakharchik, D. Blume, S. Giorgini, and B. Granger, J. Phys. B: At. Mol. Opt. Phys. **37**, S205 (2004).
[12] J. L. DuBois, Ph.D. thesis, University of Delaware, 2002.
[13] T. Kinoshita, T. Wenger, and D. S. Weiss, Science **305**, 1125 (2004).
[14] T. Kinoshita, T. Wenger, and D. S. Weiss, Phys. Rev. Lett. **95**, 190406 (2005).
[15] B. Paredes, A. Widera, V. Murg, O. Mandel, S. Fölling, I. Cirac, G. V. Shlyapnikov, T. W. Hänsch, and I. Bloch, Nature (London) **429**, 277 (2004).
[16] F. Meinert, M. Panfil, M. J. Mark, K. Lauber, J.-S. Caux, and H.-C. Nägerl, Phys. Rev. Lett. **115**, 085301 (2015).
[17] I. Bloch, *Quantum Matter at Ultralow Temperatures* (IOS Press, Amsterdam, 2016).
[18] D. S. Petrov, G. V. Shlyapnikov, and J. T. M. Walraven, Phys. Rev. Lett. **85**, 3745 (2000).
[19] M. Cazalilla, R. Citro, T. Giamarchi, E. Orignac, and M. Rigol, Rev. Mod. Phys. **83**, 1405 (2011).
[20] G. Astrakharchik, Ph.D. thesis, Facolt'a di Scienze Matematiche Fisiche e Naturali, Universit'a degli Studi di Trento, 2004.
[21] H. J. Ryser, *Combinatorial mathematics*, Vol. 14 (JSTOR, New York, 1963).
[22] C. D. Godsil, J. Graph Theor. **5**, 285 (1981).
[23] T. Tao and V. Vu, Adv. Mathematics **220**, 657 (2009).
[24] L. H. Thomas, P. Camb. Philos. Soc. **23**, 542 (1927).
[25] E. Fermi, Rend. Accad. Naz. **6**, 602 (1927).
[26] L. Tisza, Nature (London) **141**, 913 (1938).
[27] P. Nozierres, in *Bose-Einstein Condensation*, edited by A. Griffin, D. W. Snoke, and S. Stringari (Cambridge University Press, Cambridge, 1995), Chap. 2, pp. 15–30.
[28] E. J. Mueller, T.-L. Ho, M. Ueda, and G. Baym, Phys. Rev. A **74**, 033612 (2006).
[29] O. Gunnarsson and B. I. Lundqvist, Phys. Rev. B **13**, 4274 (1976).
[30] D. C. Langreth and J. P. Perdew, Phys. Rev. B **15**, 2884 (1977).
[31] L. Landau, Phys. Rev. **60**, 356 (1941).
[32] O. Penrose and L. Onsager, Phys. Rev. **104**, 576 (1956).